

Article

Critical Energy Properties Study for Unsymmetrical Deformable Structures

Leonid Stupishin * and Vladimir Mondrus

Department of Theoretical and Structural Mechanics, Institute of Construction and Architecture, National Research Moscow State University of Civil Engineering, 26, Yaroslavskoe Shosse, 129337 Moscow, Russia; mondrusvl@mgsu.ru

* Correspondence: stupishinlyu@mgsu.ru

Abstract: There are difficulties in the formulation and solution of problems for follower loading, temperature actions, and whether the Lagrange principle is used. By dividing the external loads and internal deformation fields that exist according to their own laws, we focused on the advantages in mechanics of deformable solids. This paper develops an approach to the study of the internal strain energy of deformed systems, based on the criterion of the critical levels of the internal strain energy. According to the criterion, the achievement of the limiting values of the internal strain energy by the system with varying internal parameters of the structure is possible for certain types of “self-stress” (“self-balance”) for deformable bodies. The latter corresponds to the levels of the critical energy of the body determined by the eigenvalues of the internal strain energy. New problems, namely the “weak link” and “progressive limiting state of the system”, are formulated and demonstrated in the examples of the study of asymmetric rod systems. The methodology used here is based on matrix methods of the structural mechanics and a mathematical apparatus for eigenvalue problems.

Keywords: self stress; resistance; limiting state; matrix methods; solid deformable body critical energy; concepts for multi-story construction



Citation: Stupishin, L.; Mondrus, V. Critical Energy Properties Study for Unsymmetrical Deformable Structures. *Buildings* **2022**, *12*, 779. <https://doi.org/10.3390/buildings12060779>

Academic Editors: Vlatka Rajčić and Chiara Bedon

Received: 23 April 2022

Accepted: 4 June 2022

Published: 7 June 2022

Publisher's Note: MDPI stays neutral with regard to jurisdictional claims in published maps and institutional affiliations.



Copyright: © 2022 by the authors. Licensee MDPI, Basel, Switzerland. This article is an open access article distributed under the terms and conditions of the Creative Commons Attribution (CC BY) license (<https://creativecommons.org/licenses/by/4.0/>).

1. Introduction

For almost half a century, formulations of problems in the mechanics of a solid deformable body, based on varying the total deformation energy of a structure, have been used often by researchers [1–10]. The use of mathematical apparatus for calculating the variations made it possible to obtain solutions to complex problems regarding the theory of stability and dynamics of structures, as well as nonlinear problems regarding the deformation of spatial systems [10–20]. A special place is occupied by numerical methods for studying complex systems operating in the nonlinear stage of deformation, based on variational formulations of problems in construction mechanics [21–35], which are the fundamentals for the creation of software systems using the finite element method, the boundary element method, and other methods of structural mechanics.

The vast majority of reports regarding the problems mentioned above are based on the Lagrange approach, where the minimum of the total energy of the system leads to the equations of the state of the system depending on the acting external loads. In this case, there may be an impression that the behavior of the system is completely determined by the magnitude, type, and law of the changes in the external load.

As noted in a number of studies [33,34], this approach does not always allow for calculating systems that are subject to follower loads, temperature, and similar influences. The necessity of formulating problems in the form of homogeneous systems of equations has been noted, on the basis of which one can then restore the form of a possible external load.

Thus, there is insufficient information on the properties of the internal strain energy of deformable systems. The hypothesis is that any deformable body has critical levels of internal strain energy (hereafter termed critical energy), where the structure can change the

form of the law of equilibrium states or the structural model, making it possible to obtain a criterion for the critical levels of internal strain energy, which are tested on a number of problems regarding the stability and bending of structures [35].

One of the most important directions in the study of structures at critical energy levels is that the theory can be used as the basis of the limit state design (LSD) of structures.

At present, the theory LSD of a structure does not have a unified theoretical mathematical base and is developing in a number of independent directions. Each of these theories is based on the hypothesis of the onset of the limit state, for which a mathematical model of the problem is formulated [36–43]. Obviously, the number of hypotheses cannot be limited; therefore, the theory of LSD is a complicated set of particular theories, which are often poorly combined with each other.

In [44,45], an approach was proposed that allowed for stating a mathematical model of problems on the limiting state of a structure uniting all possible formulations of ultimate limit state (ULS), including the serviceability limit state (SLS).

2. Methods

The internal strain energy for the deformation of the structural system in matrix form can be represented as follows

$$2U = \{\xi\}^T [K] \{\xi\} = \{\Phi\}_{in}^T [L] \{\Phi\}_{in} \quad (1)$$

where U is the internal strain energy of the structure, $\{\xi\}$ is the generalized displacement vector, $\{\Phi\}_{in}$ is the generalized forces vector, $[K]$ is the stiffness matrix, $[L]$ is the flexibility matrix, T denotes transposition.

Thus, it is easy to see that the levels of the internal strain energy of deformation are determined by the values of the stiffness (flexibility) matrices of the system.

In [44], the equations of the state of a system with lumped parameters at critical energy levels were obtained, written in the matrix form

$$[L] \{\delta\Phi_k^{in}\} = [\lambda_0^L] \{\delta\Phi_k^{in}\} \quad (2)$$

where $[\lambda_0^L]$ is the matrix of the eigenvalues for the flexibility matrix. The eigenvalues λ_{0i}^L are the main values of the flexibility of the structure, and the eigenvectors $\{\delta\Phi_K^{in}\}$ are the amplitude values of the distribution of self-stress forces.

For variations of nodal displacements (structural system reactions), the relation for the eigenvalues of the flexibility and stiffness matrices is valid

$$[\lambda_0^K] = [\lambda_0^L]^{-1} \quad (3)$$

here, λ_0^K are the eigenvalues of the stiffness matrix of the system.

The physical meaning derived from Equations (1) and (2) is the state of self-stress in a statically indeterminate system at critical energy levels. The solution of the eigenvalue problem gives the main nodal structure displacements and the corresponding vectors of the amplitude values of the nodal reaction forces of the structure.

Matrix expressions of the force method and the displacement method are consequences of the expressions for the stationarity of the internal energy of the structure (1)

$$[K] \{\xi\} = \{\Phi\}_{ex}; [L] \{\Phi\}_{in} = \{\xi\} \quad (4)$$

Matrix operators $[K]$ and $[L]$ are the vector of unknown nodal displacements which are converted into a vector of the nodal structure generalized reactions and the vector of internal forces in the structure elements into a vector of nodal generalized displacements, respectively. In this case, the directions of the vectors of external nodal loads and displacements are generally different and have different angles with respect to the original axes.

At the same time, the extreme (main) directions of nodal generalized displacements and generalized reactions are always orthogonal to each at the same angles as the original axes. Thus, we can write

$$\begin{aligned} [\lambda_{\min}^K] \{\vartheta^K\} &= \{R_{\min}^{\max}\} \\ [\lambda_{\max}^L] \{\vartheta^L\} &= \{Z_{\max}^{\min}\} \end{aligned} \quad (5)$$

where $\{R_{\min}^{\max}\}$ is the minimum or maximum value of the generalized reaction system to the external load, and $\{Z_{\max}^{\min}\}$ is the maximum or minimum nodal generalized displacement corresponding to the generalized reactions. Vectors $\{R_{\min}^{\max}\}$ and $\{Z_{\max}^{\min}\}$ are mutually perpendicular, which enables assessing the values of the limiting stiffness and flexibility of the system and to make a comparison with the acting load.

For example, the solution to the problem of finding the minimum and maximum values of the limiting reactions of the system, which is opposed to the external load, can be represented in the form of two circles limiting the area of the system's $\{R\}$ reactions, as shown in Figure 1.

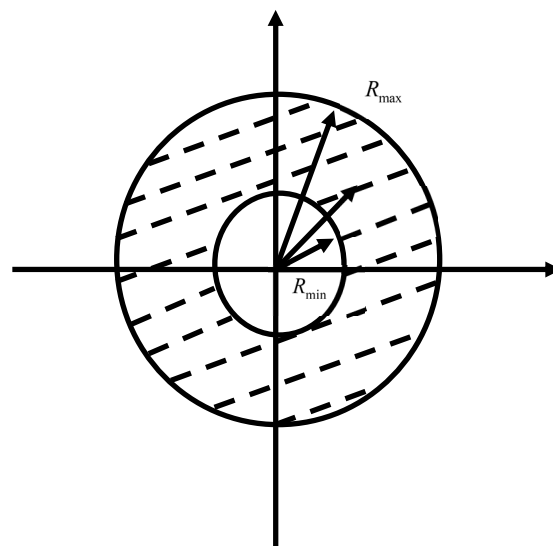


Figure 1. The area of the system's limiting states.

The value $\{R\}_{\min}$ limits the area within which the limiting state of the system is impossible due to the negligibly small reaction (allowable external forces) values. R_1 —is the reaction vector of the structure determining a point inside the circles of limit states that does not lie on the line of max (min) limit states value. Starting from the value of the reactive stiffness of the system $\{R\}_{\min}$, the onset of the limiting state is possible in one or several elements of the structure. At the value of reactive stiffness $\{R\}_{\max}$, the system has minimum stiffness and maximum flexibility $\{Z_{\min}\}$. The values of the internal forces (deformations) have the maximum allowable values.

We may obtain the same unit values for $\{R\}_{\max}$ and $\{Z_{\min}\}$ vectors when normalizing to the maximum value. The normalized values of the reactions (deformations) coincide for the eigenvalues of the stiffness and flexibility matrices of the system.

The Lagrange principle, as the base of the traditional calculation methods, puts the system reactions vector $\{R\}_1 = \{P_1\}$ in agreement with the external load. Obviously, with this approach, not all of the bearing capacity of the system has been exhausted, only a part of it. The structure, in the worst case, lost part of the links (part of the resistance), but remains geometrically unchanged and can bear an increasing load.

Critical Energy Levels of a Non-Symmetric Rod System

To study the processes of changing the internal potential energy of an elastic non-symmetric structure, the three-rod system considered is shown in Figure 2.

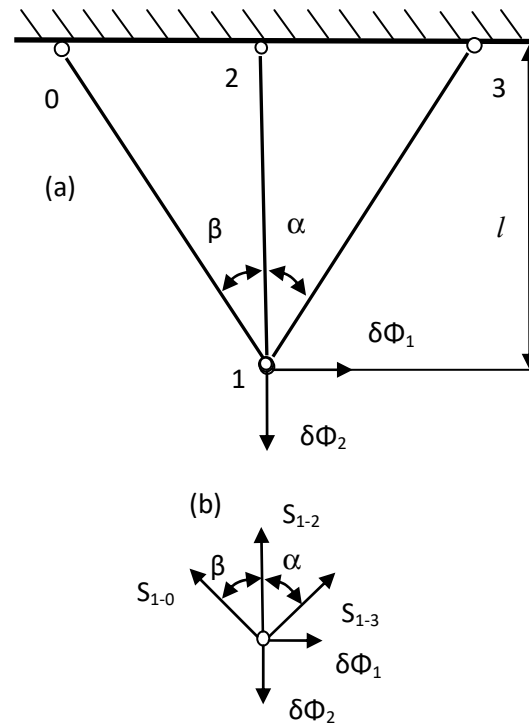


Figure 2. Three-rod system: (a) design scheme and (b) node 1.

For simplicity, we will take the same values for the stiffness of the rods $\eta_1 = \eta_2 = \eta_3 = 1$, $\eta_i = EA/E_i A_i$, elastic moduli E , and cross-sectional areas A . Inclined rods are located at the corners $\alpha = \pi/4$, $\beta = \pi/3$. We will assume that the system works in the elastic stage until the first critical level of internal potential energy is reached.

Flexibility matrix of the rod structure

$$[L] = \frac{l}{EA} \begin{vmatrix} 1.397 & 0.1295 \\ 0.1295 & 0.6883 \end{vmatrix} \quad (6)$$

The eigenvalue problem solution gives us the eigenvectors

$$[\vartheta^L] = \begin{vmatrix} 0.9847 & -0.1743 \\ 0.1743 & 0.9847 \end{vmatrix} \quad (7)$$

and the eigenvalues of the flexibility matrix

$$[\lambda^L] = \frac{l}{EA} \begin{vmatrix} 1.4199 & 0 \\ 0 & 0.6654 \end{vmatrix} \quad (8)$$

The stiffness matrix of the rod structure has the form

$$[K] = \frac{EA}{l} \begin{vmatrix} 0.7285 & -0.137 \\ -0.137 & 1.4785 \end{vmatrix} \quad (9)$$

Corresponding to the eigenvalues of the stiffness matrix

$$[\lambda^K] = \frac{EA}{l} \begin{vmatrix} 0.7043 & 0 \\ 0 & 1.5028 \end{vmatrix} \quad (10)$$

Eigenvectors of the stiffness matrix

$$[\vartheta^K] = \begin{bmatrix} -0.9847 & 0.1743 \\ -0.1743 & -0.9847 \end{bmatrix} \quad (11)$$

Figure 3 shows the external stiffness ellipse and the external flexibility ellipse of the system presented in a dimensionless form.

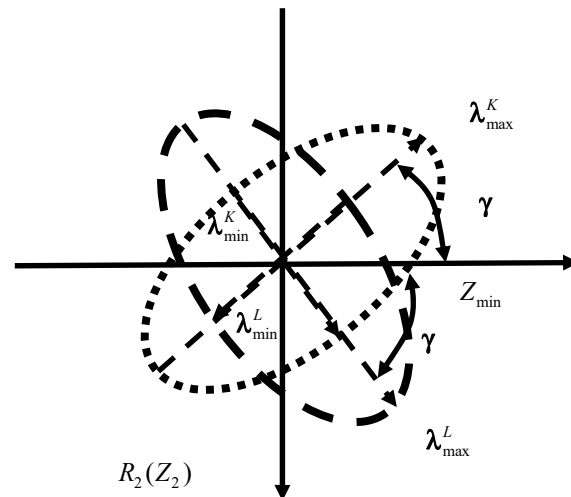


Figure 3. Stiffness ellipse (dots) and flexibility ellipse (dotted line) of an asymmetrical statically indeterminate system.

The maximum radius value of the flexibility ellipse is the reciprocal of the minimum radius value of the stiffness ellipse, and the minimum radius value of the flexibility ellipse is the reciprocal of the maximum radius value of the stiffness ellipse. Therefore, by normalizing the eigenvalues of the flexibility and stiffness ellipses according to the maximum eigenvalues, we can obtain the same values of the radii value of the ellipses $\lambda_{\max}^L = \lambda_{\max}^K = 1, \lambda_{\min}^L = \lambda_{\min}^K = 0.4686$ regarding the problem under consideration. The extreme displacements (reactions) of the system has projections on the initial directions of the axes in the form $\{Z_{\max}^{1,2}\} = \lambda_{\max}^L \{\vartheta^L\}$ (see Figure 4). Because the system has only two degrees of freedom at node 1, it is possible to construct ellipses of the limiting lines of rigidity and flexibility of the non-symmetric rod structure, corresponding to the first critical energy level of the structure.

If the projections of the external displacements of the nodes on the axis are greater than $Z_{\max}^{1,2}$, the system is overloaded, that is, either it has lost some of the links or is geometrically changeable. The condition of allowable nodal displacements follows from the geometric relationships of the ellipse.

$$Z_a \leq \frac{Z_{\max} Z_{\min}}{\sqrt{Z_{\max} \sin \varphi + Z_{\min} \cos \varphi}} \quad (12)$$

The condition for the allowable loads will be written in the same way.

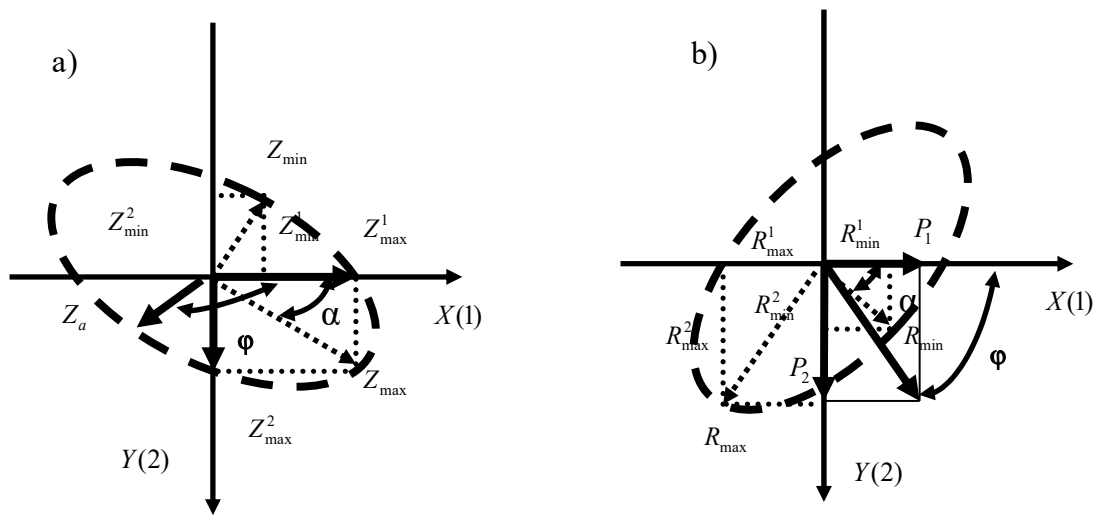


Figure 4. The ellipse of the external flexibility of the system (a) and the ellipse of the external rigidity of the system (b) for the first state of self-tension.

Internal forces in the truss rods from the external loads can be calculated by

$$[S] = [B]^{-1}[A]^T[L]\{P\} \tag{13}$$

and from the reaction of the system to variations of the external influences according to the formula

$$[S] = [C][A]^T[\lambda^L]\{\vartheta_{\max,\min}^L\} \tag{14}$$

The calculation results are given in Table 1.

Table 1. Internal forces in the rods of the system from the nodal external and reactive forces.

Bars Forces	External Force $P_1 = 1$	External Force $P_2 = 1$	Total Action of the Forces $P_1 + P_2$	System Response R_1^{\max}	System Response R_2^{\max}	System Response R_{\max}	System Response R_{\min}
1	2	3	4	5	6	7	8
S_{1-0}	0.6373	0.2282	0.8654	0.8909	0.1495	0.9475	0.07558
S_{1-2}	0.1295	0.6883	0.8178	0.181	0.451	0.3514	0.436
S_{1-3}	-0.6337	0.2794	-0.354	-0.886	0.1831	-0.8169	0.2566

Here, the action of the external and reactive forces of the system was taken in one direction, so that it would be more convenient to compare the results. The values of the largest forces in the rods caused by the external load (column 4) were in the interval between the values of the forces caused by the maximum (column 7) and minimum (column 8) reactive forces of the system for two types of self-stress. If we compare the maximum values of the forces arising in rod 0–1 (columns 2 and 5), for the case of the action of forces in the direction of axis 1, then we have a margin of strength in terms of efforts equal to 39.8%. If we assume that the unit external forces act on the system in the direction of two axes at the same time, then the strength margin for internal forces (see columns 4 and 7) in the structure rods will be 9.5%. Obviously, these two cases are very rare in practice. The more likely is the case when the projections of the load vector add up to a unit vector is realized, for example, with simple loading. Then, the difference between the load vector and the reaction vector of the system will be the value of the maximum eigenvalue. The same can be said about the internal forces in the structural rods from these two loads.

For the problem to be solved, the eigenvalues increase with decreasing angles of inclination of the rods with the same areas of the rods. The minimum eigenvalues are observed at inclination angles of the rods close to 45° .

If the system has the same angles of inclination as the rods, and the areas of the inclined rods differ, and the eigenvalues of the system follow a similar relationship.

3. Results

3.1. Tasks for Checking Strength (Structural Analysis)

Example 1:

The system shown in Figure 2 has the following specified geometric parameters: $l = 2$ m, $\alpha = 60^\circ$, $\beta = 45^\circ$, $\eta_2 = 1$, $\eta_1 = 1.457\eta_2$, $\eta_3 = 2.778\eta_2$, $A_{1-0} = A_1 = 0.5388 \cdot 10^{-4}$ m², ($d = 8.3$ mm), $A_{1-2} = A_2 = 0.785 \cdot 10^{-4}$ m², ($d = 10$ mm), $A_{1-3} = A_3 = 0.2826 \cdot 10^{-4}$ m², ($d = 6.0$ mm) and mechanical characteristics of the material of $E = 2.1 \cdot 10^5$ MPa, $\sigma_t = 240$ MPa. Check the bearing capacity with an external load given by the projections on the axis $P_1 = 10$ kN, $P_2 = 20$ kN.

Determine the allowable load under the condition that one or more rods reach the limit state due to the attainment of the yield stresses.

Determine the ultimate load on the system, which turns it into a mechanism.

Solution 1: Comparison of the external load and system response to variations in the external forces.

(1). Determine the modulus of the external load vector and the angle of inclination of the resultant to the axis $P = \sqrt{20^2 + 10^2} = 22.36$ kN, $\text{tg}\varphi = 20/10 = 2$, $\varphi = 63.43^\circ$, $\bar{P} = P/22.36 = 1.0$.

(2). We calculated the values of the radii of the limiting state ellipse (Figure 4).

For the stiffness matrix rod structure

$$[K] = \frac{EA}{l} \begin{vmatrix} 0.3846 & 0.02133 \\ 0.02133 & 1.213 \end{vmatrix} \quad (15)$$

calculating eigenvalues

$$[\lambda^K] = \frac{EA}{l} \begin{vmatrix} 0.384 & 0 \\ 0 & 1.214 \end{vmatrix} \quad (16)$$

and eigenvectors

$$[\vartheta^K] = \begin{vmatrix} -0.9997 & -0.02572 \\ 0.02572 & -0.9997 \end{vmatrix} \quad (17)$$

We determined the allowable value of the reactive force for the direction of the equally effective external load $R_{\max} = 1.213\vartheta^K A_2 E/l$, $R_{\min} = 0.3846\vartheta^K A_2 E/l$. Then, we have $\vartheta^K = \sigma_t/0.3846E$. The values of the reactive components of the system are $R_{\max} = 3.154\sigma_t A_2$, $R_{\min} = \sigma_t A_2$. The values of the eigenvectors for the main axes of the rigidity of the system are rotated by 90° with respect to the original axes, and the R_{\max} direction and R_{\min} are mutually perpendicular.

We found the dimensionless value of the allowable load according to (12), per unit of movement of the system node, and with the same direction as the given load $\bar{P}_a = 1.945$. Here $\bar{P}_a = P_a/\sigma_t A_2$.

Then, the largest value of the reactive nodal force created by the system in the direction of the acting external load will be $P_a = \sigma_t A_1 = 36.64$ kN.

The value of the resulting specified external load $P = 22.36$ kN, which is less than the allowed value. The system will not lose resistance. According to the condition of the problem, this means that there is a margin of safety for the load (or residual resource of the resistance), and the structure can be subjected to an optimization procedure.

Solution 2: Comparison of the forces in the rods from a given normalized load and the forces detected during self-tension of the system.

We normalized the external load by the resulting value and obtained a vector of external influences in the form $\{\bar{P}\} = \{P\}/22.36 = \{0.4472, 0.8945\}^T$.

Calculate the flexibility matrix of the structure

$$[L] = \frac{l}{EA} \begin{vmatrix} 2.602 & -0.04576 \\ -0.04576 & 0.824 \end{vmatrix} \quad (18)$$

define eigenvalues

$$[\lambda^L] = \frac{l}{EA} \begin{vmatrix} 2.604 & 0 \\ 0 & 0.824 \end{vmatrix} \quad (19)$$

and vector-matrix of eigenvectors

$$[\vartheta^L] = \begin{vmatrix} 0.9997 & 0.02572 \\ -0.02572 & 0.9997 \end{vmatrix} \quad (20)$$

We determined the internal forces in the rods of the system from the normalized vector of the external load using the formula

$$[S_P] = -[C][A]^T[L]\{\bar{P}\} \quad (21)$$

We obtained the distribution of efforts from the dimensionless components of the external load vector in the form

$$[\bar{S}^P] = \begin{vmatrix} 0.4568 \\ 0.7177 \\ -0.07294 \end{vmatrix} \quad (22)$$

We found the vector of internal efforts from the nodal reaction vector of the system

$$[\bar{S}_{\delta\Phi_{in}}] = \begin{vmatrix} 2.106 \\ 0.5044 \\ -1.132 \end{vmatrix} \quad (23)$$

From the results obtained, it follows that the force in rod 2-1 from the external load is greater than the force from the self-tension in the same rod $\bar{S}_{2-1}^P > \bar{S}_{2-1}^{\delta\Phi_{in}}$. Therefore, the specified bar must lose resistance from a given load.

Compared efforts can be presented in dimensional units. The internal force from the external load in rod 2-1 is $S_{0-1}^P = 0.7177 \cdot P = 16.05$ kN.

The magnitude of the force in the same rod from the nodal reaction of the system is $S_{0-1}^{\delta\Phi_{in}} = 0.5044\sigma_t A = 9.503$ kN.

The permissible maximum value of the force in the rod from the value of the reaction of the system is less than the force from a given load on 6.55 kN.

Solution 3: Comparison of stresses in rods from a given load and allowable stresses (design resistances) according to the traditional method.

According to the matrix structural mechanics algorithm, we have the formula

$$[S] = -[C][A]^T[L]\{P\} \quad (24)$$

Load vector $\{P\} = \{10; 20\}$ (kN).

Determine internal forces in rods and structures in (kN)

$$[S] = \begin{vmatrix} 10.22 \\ 16.05 \\ 1.631 \end{vmatrix} \quad (25)$$

The stress in the most loaded bar is $\sigma_{1-0}^{cr} = S_{1-0}^{cr}/A = 204.4 \text{ MPa}$, which is less than the yield stress of the rod material. That is, the bar and the system have no loss of resistance.

3.2. Cross-Section Sizing Tasks (Structural Design)

Example 2:

For the system shown in Figure 2, with geometric parameters $l = 2 \text{ m}$, $\alpha = 60^\circ$, $\beta = 45^\circ$, modulus of elasticity $E = 2.1 \cdot 10^5 \text{ MPa}$, and yield point $\sigma_t = 240 \text{ MPa}$, select the area of a rod of circular cross-section from a given load $P_1 = 10 \text{ kN}$, $P_2 = 20 \text{ kN}$.

Solution 1: Traditional method of strength of materials.

Based on the results obtained in Section 3.1 Solution 3, we obtained $A = S_{1-0}^{cr}/\sigma_t = 0.6688 \cdot 10^{-4} \text{ m}^2$.

We obtained the diameter of the rod as $d = 9.2 \text{ mm}$.

Solution 2: The use of forces in the rods from the normalized values of the load.

For the obtained value of the forces in the rods, we found the cross-sectional area $A = 0.6688 \cdot 10^{-4} \text{ m}^2$.

3.3. The Weak Link (WL) Problem

Let us solve example 1 under the assumption that the rods have decreased in diameter by 0.8 mm.

Then, according to solutions of examples 1 and 2, we can conclude that in the middle bar 1–2, the limiting state reached the yield condition of the bar.

Note that because of the formulation of the problem in the form of finding the stress state of self-stress in a structure at a critical energy level, we have the opportunity to find a rod in which the greatest efforts (stresses) will appear first.

We will call this problem statement the “weak link” (WL) problem.

3.4. Problem of the Progressive Limit State Design (PLSD) of the Structure

Let us find out which rod will lose its resistance next. In the case of a large number of elements in the system, it is possible to find the sequence of the exit of elements from the work to the load because of the onset of the limiting state. We will call this type of problem the problem of a progressive limit state design.

To do this, consider the two-rod structure shown in Figure 5.

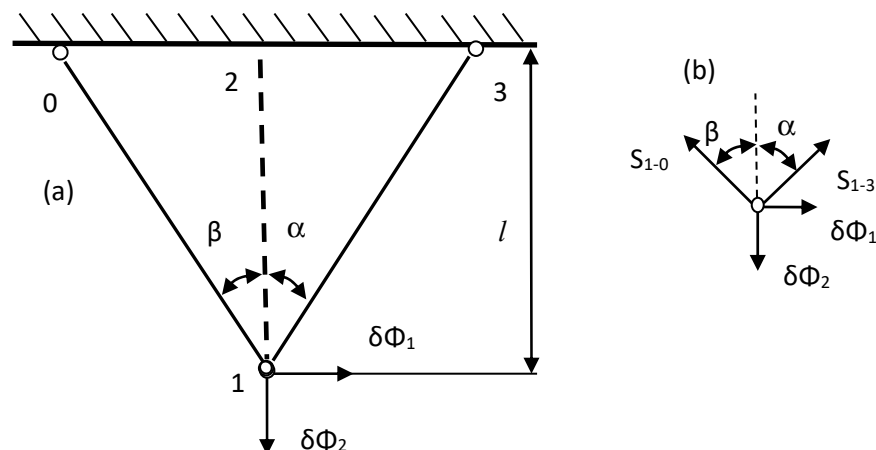


Figure 5. Three-rod system without the middle bar removed: (a) design model and (b) node 1.

The stiffness matrix two-rod structure has the form

$$[K] = \frac{EA}{l} \begin{vmatrix} 0.3846 & 0.02133 \\ 0.02133 & 0.2131 \end{vmatrix} \quad (26)$$

Determining eigenvalues

$$[\lambda^K] = \frac{EA}{l} \begin{vmatrix} 0.3872 & 0 \\ 0 & 0.2104 \end{vmatrix} \quad (27)$$

and eigenvectors

$$[\vartheta^K] = \begin{vmatrix} 0.9926 & -0.1215 \\ 0.1215 & 0.9926 \end{vmatrix} \quad (28)$$

We determined the efforts from the reaction of the system $\bar{S}_{1-0}^R = -1.185$, $\bar{S}_{1-3}^R = -0.8632$.

We compared these with the efforts from the normalized external load vector $\bar{S}_{1-0}^P = 0.9822$, $\bar{S}_{1-3}^P = 0.5705$.

For two cases, we found that the next one to go out of work on the load was the rod 0–1.

We determined the actual cross-sectional area of the rod 0–1 after corrosion $d = 7.5$ mm. We obtained $A = 3.14 \cdot 7.5^2/4 = 0.4416 \cdot 10^{-4} \text{ m}^2$.

The stresses in the bar from the limiting value of the reaction of the structure were $\sigma_{1-0}^R = 284.4$ MPa.

The stresses in the bar from a given external load were $\sigma_{1-0}^R = \sigma_{1-0}^P = 497.3$ MPa.

The rod lost strength in the plastic stage of deformation.

4. Conclusions

The study of the critical levels of strain energy based on the concept of “self-stress” or “self-balance” of a structure permit us to find its limiting state.

Both the limiting states (ULS and SLS) are investigated as single mathematical model using the eigenvalues problem of the stiffness (deflections) matrices.

Bringing the stiffness properties of the system to certain nodes and through the calculation of the nodal reactions of the structure (or nodal displacements), we can construct hyper ellipsoids of restrictions allowing for displacements (nodal forces) arising in the structure. The restriction surface lets us discover the external loads before determining the stresses in the elements of the structure.

The proposed approach enables finding the bar (link), which first has a loose resistance at any loading of the structure. This is the formulation of the problem regarding the WL finding.

The sequential application of the problem of the WL makes it possible to construct a methodology for the progressive limiting state design of the structure, when the designer has the opportunity to reproduce the process of the sequential failure of structural elements affected by beyond design basis or accidental action.

In spite of using the new formulation, the results obtained for the new examples were identical to those from the classical methods of structural mechanics yields.

Thus, the proposed methodology makes it possible to formulate and solve new types of problems in structural mechanics, such as progressive collapse, controlling the parameters of the system under beyond design basis actions, and smart structures.

Author Contributions: Conceptualization, L.S. and V.M.; methodology, L.S.; validation, L.S. and V.M.; formal analysis, L.S.; resources, V.M.; writing—original draft preparation, L.S.; writing—review and editing, V.M. All authors have read and agreed to the published version of the manuscript.

Funding: This research received no external funding.

Institutional Review Board Statement: Not applicable.

Informed Consent Statement: Not applicable.

Data Availability Statement: Not applicable.

Conflicts of Interest: The authors declare no conflict of interest.

References

1. Gurtin, M.E. Variational Principles for Linear Elastodynamics. *Arch. Ration. Mech. Anal.* **1964**, *16*, 34–50. [[CrossRef](#)]
2. Prager, W. Variational principles for elastic plates with relaxed continuity requirements. *Int. J. Solids Struct.* **1968**, *4*, 837–844. [[CrossRef](#)]
3. Finlayson, B.A. Existence of Variational Principles for the Navier-Stokes Equation. *AIP Phys. Fluids. Phys. Fluids* **1972**, *15*, 963–967. [[CrossRef](#)]
4. Reddy, J. Variational principles for linear coupled dynamic theory of thermoviscoelasticity. *Int. J. Eng. Sci.* **1976**, *14*, 605–616. [[CrossRef](#)]
5. Arthurs, A.M.; Jones, M.E. On Variational Principles for Linear Initial Value Problems. *J. Math. Anal. Appl.* **1976**, *54*, 840–845. [[CrossRef](#)]
6. Van Groesen, E.W.C. Variational methods in mathematical physics. *Tech. Hogesch. Eindh.* **1978**, *216*. [[CrossRef](#)]
7. Anderson, I.M.; Duchamp, T. On the existence of global variational principle. *Am. J. Math.* **1980**, *102*, 781–786. Available online: <http://www.jstor.org/stable/2374195> (accessed on 27 September 2011). [[CrossRef](#)]
8. Washizu, K. *Variational Methods in Elasticity and Plasticity*; Pergamon Press: Oxford, UK, 1982; Volume 542.
9. Auchmuty, G. Duality for Non-Convex Variational Principles. *J. Differ. Equ.* **1983**, *50*, 80–145. [[CrossRef](#)]
10. Berdichevsky, V.L. *Variational Principles of Continuum Mechanics*; Springer: Berlin/Heidelberg, Germany, 2009; p. 1011.
11. Bathe, K.J. *Finite Element Procedures*; Prentice Hall: Hoboken, NJ, USA, 2004; p. 1043.
12. Angelis, F.; Cancellara, D. Multifield variational principles and computational aspects in rate plasticity. *Comput. Struct.* **2017**, *180*, 27–39. [[CrossRef](#)]
13. Reddy, J.N. *Energy Principles and Variational Methods in Applied Mechanics*; Wiley: Hoboken, NJ, USA, 2017; p. 760. [[CrossRef](#)]
14. Renaud, A.; Heuzé, T.; Stainier, L. The discontinuous Galerkin material point method for variational hyperelastic–plastic solids. *Comput. Methods Appl. Mech. Eng.* **2020**, *365*, 112987. [[CrossRef](#)]
15. Nairn, J.A.; Hammerquist, C.C.; Smith, G.D. New material point method contact algorithms for improved accuracy, large-deformation problems, and proper null-space filtering. *Comput. Methods Appl. Mech. Eng.* **2020**, *362*, 112859. [[CrossRef](#)]
16. Coombs, W.M.; Augarde, C.E.; Brennan, A.G.; Brown, M.J.; Charlton, T.J.; Knappett, J.A.; Motlagh, Y.G.; Wang, L. On Lagrangian mechanics and the implicit material point method for large deformation elasto-plasticity. *Comput. Appl. Mech. Eng.* **2020**, *358*, 112622. [[CrossRef](#)]
17. Portillo, D.; Oesterle, B.; Thierer, R.; Bischoff, M.; Romero, I. Structural models based on 3D constitutive laws: Variational structure and numerical solution. *Comput. Methods Appl. Mech. Eng.* **2020**, *362*, 112872. [[CrossRef](#)]
18. Wang, X.; Xu, Q.; Atluri, S.N. Combination of the variational iteration method and numerical algorithms for nonlinear problems. *Appl. Math. Model.* **2019**, *79*, 243–259. [[CrossRef](#)]
19. Samaniego, E.; Anitescu, C.; Nguyen-Thanh, V.M.; Guo, H.; Hamdia, R.; Zhuang, X.; Rabczuk, K. An energy approach to the solution of partial differential equations in computational mechanics via machine learning: Concepts, implementation and applications. *Comput. Methods Appl. Mech. Eng.* **2020**, *362*, 112790. [[CrossRef](#)]
20. Ba, K.; Gakwaya, A. Thermomechanical total Lagrangian SPH formulation for solid mechanics in large deformation problems. *Comput. Methods Appl. Mech. Eng.* **2018**, *342*, 458–473. [[CrossRef](#)]
21. Bai, L.; Wadee, M.A.; Köllner, A.; Yang, J. Variational modelling of local–global mode interaction in long rectangular hollow section struts with Ramberg–Osgood type material nonlinearity. *Int. J. Mech. Sci.* **2021**, *209*, 106691. [[CrossRef](#)]
22. Yang, S.; Shi, W.; Chen, Z.; Qian, C.; Yang, C.; Hang, L. Composite mechanics and energy method based stiffness prediction model for composite leaf springs. *Mech. Based Des. Struct. Mach.* **2019**, *47*, 375–386. [[CrossRef](#)]
23. Wu, Y.; Fu, L.; Wu, W.; Cao, Y.; Zhou, X. Nonlinear Stress Analysis of Flexible Pile Composite Foundation by Energy Method. *Adv. Mater. Sci. Eng.* **2018**, *2018*, 8176398. [[CrossRef](#)]
24. Lin, Y.; Zhang, X.; Xu, W.; Zhou, M. Importance Assessment of Structural Members Based on Elastic-Plastic Strain Energy. *Adv. Mater. Sci. Eng.* **2019**, *2019*, 8019675. [[CrossRef](#)]
25. Xiang, C.; Li, C.; Zhou, Y.; Dang, C. An Efficient Damage Identification Method for Simply Supported Beams Based on Strain Energy Information Entropy. *Adv. Mater. Sci. Eng.* **2020**, *2020*, 9283949. [[CrossRef](#)]
26. Nguyen, P.; Lea, C. Failure analysis of anisotropic materials using computational homogenised limit analysis. *Comput. Struct.* **2021**, *256*, 17. [[CrossRef](#)]
27. Huang, Y.; Karami, B.; Shahsavari, D. Static stability analysis of carbon nanotube reinforced polymeric composite doubly curved micro-shell panels. *Archiv. Civ. Mech. Eng.* **2021**, *21*, 139. [[CrossRef](#)]
28. Yue, X.; Yue, X.; Borjalilou, V. Generalized thermoelasticity model of nonlocal strain gradient Timoshenko nanobeams. *Archiv. Civ. Mech. Eng.* **2021**, *21*, 124. [[CrossRef](#)]
29. Yang, Z.; Lu, H.; Sahmani, S. Isogeometric couple stress continuum-based linear and nonlinear flexural responses of functionally graded composite microplates with variable thickness. *Archiv. Civ. Mech. Eng.* **2021**, *21*, 114. [[CrossRef](#)]
30. Wang, G.; Zhang, Y.; Arefi, M. Three-dimensional exact elastic analysis of nanoplates. *Archiv. Civ. Mech. Eng.* **2021**, *21*, 91. [[CrossRef](#)]
31. Moayyedean, F.; Kadkhodayan, M. Modified Burzynski criterion along with AFR and non-AFR for asymmetric anisotropic materials. *Archiv. Civ. Mech. Eng.* **2021**, *21*, 64. [[CrossRef](#)]

32. Zhu, L.; Wang, J.J.; Li, M.J. Finite beam element with 22 DOF for curved composite box girders considering torsion, distortion, and biaxial slip. *Archiv. Civ. Mech. Eng.* **2020**, *20*, 101. [[CrossRef](#)]
33. Alfutov, N.A. *Osnovy Rascheta na Ustoichivost Uprugih System [Basics of Calculating the Stability of Elastic Systems]*. 1991, p. 336. Available online: <https://booksee.org/book/1007295> (accessed on 23 June 2009). (In Russian).
34. Bryan, G.H. On the Stability of a Plane Plate Under Thrusts in Its Own Plane, with Applications to the 'Buckling' of the Sides of a Ship. *Proc. Lond. Math. Soc.* **1891**, *22*, 54–67. [[CrossRef](#)]
35. Stupishin, L.Y. Variational criteria for critical levels of internal energy of a deformable solid. *Appl. Mech. Mater.* **2014**, 578–579, 1584–1587. [[CrossRef](#)]
36. Yang, Y.; Gao, F.; Cai, C. A Novel Polyaxial Strength Criterion for Rock Materials under General Stress Condition. *Int. J. Appl. Mech.* **2018**, *10*, 1850082. [[CrossRef](#)]
37. Perelmuter, A.; Kabantsev, O. About the Problem of Analysis Resistance Bearing Systems in Failure of a Structural Element. *Int. J. Comput. Civ. Struct. Eng.* **2018**, *14*, 103–113. [[CrossRef](#)]
38. Shanyavskiy, A.; Soldatenkov, A. The fatigue limit of metals as a characteristic of the multimodal fatigue life distribution for structural materials. *Procedia Struct. Integr.* **2019**, *23*, 63–68. [[CrossRef](#)]
39. Jamadin, A.; Ibrahim, Z.; Jumaat, M.; Hosen, M. Serviceability assessment of fatigued reinforced concrete structures using a dynamic response technique. *J. Mater. Res. Technol.* **2020**, *9*, 4450–4458. [[CrossRef](#)]
40. Atutis, E.; Atutis, M.; Budvytis, M.; Valivonis, J. Serviceability and Shear Response of RC Beams Prestressed with a Various Types of FRP Bars. *Procedia Eng.* **2017**, *172*, 60–67. [[CrossRef](#)]
41. Yu-hang, W.; Wang, W.; Jie, Y. Ultimate bearing capacity correlation of steel tube confined RC column under combined compression-bending-torsion load. *Thin-Walled Struct.* **2019**, *145*, 106408. [[CrossRef](#)]
42. Montuori, R.; Nistri, E.; Piluso, V. Thin-Walled Structures Ultimate behaviour of high-yielding low-hardening aluminium alloy. *Thin-Walled Struct.* **2020**, *146*, 106463. [[CrossRef](#)]
43. Hun, D.; Jin, S.; Seung, M. Ultimate limit state-based design versus allowable working stress-based design for box girder crane structures. *Thin Walled Struct.* **2019**, *134*, 491–507. [[CrossRef](#)]
44. Stupishin, L.Y. Limit state of building structures and critical energy levels. *Promyshlennoe I Grazhdanskoe Stroit. Ind. Civ. Eng.* **2018**, *10*, 102–106. (In Russian)
45. Stupishin, L.Y.; Moskevich, M.L. The problem of determining the «weak link» based on the internal energy critical levels of the construction. *Izv. Vuzov. Stroit. News High. Educ. Inst. Constr.* **2021**, *2*, 11–23. (In Russian) [[CrossRef](#)]